

Quantum computation with Jaynes-Cummings model

Hiroo Azuma

Institute of Computational Fluid Dynamics, 1-16-5 Haramachi, Meguro-ku,
Tokyo 152-0011, Japan

E-mail: hiroo.azuma@m3.dion.ne.jp

Abstract. In this paper, we propose a method for building a two-qubit gate with the Jaynes-Cummings model (JCM). In our scheme, we construct a qubit from a pair of optical paths where a photon is running. Generating Knill, Laflamme, and Milburn's nonlinear sign-shift gate by the JCM, we construct the conditional sign-flip gate, which works with small error probability in principle. We also discuss two experimental setups for realizing our scheme. In the first experimental setup, we make use of coherent lights to examine whether or not our scheme works. In the second experimental setup, an optical loop circuit made out of the polarizing beam splitter and the Pockels cell takes an important role in the cavity.

PACS numbers: 03.67.Bg, 32.80.-t, 42.50.Pq, 42.50.Ex

Submitted to: *J. Phys. A: Math. Gen.*

1. Introduction

Since Shor's quantum algorithm for factoring large integers more efficiently than classical algorithms appeared [1], many researchers have been devoting themselves to realization of quantum computation in their laboratories. To implement a quantum computer, we have to prepare quantum bits (qubits), which are two-state quantum systems, and quantum logic gates, which apply unitary transformations to qubits. In general, we can apply an arbitrary unitary transformation to a single qubit at ease no matter which physical system we choose as the qubit. However, almost all the researchers think implementation of a two-qubit gate to be very difficult because it has to generate nonlocal quantum correlation (entanglement) between two local qubits. Furthermore, it is shown that we can construct any unitary transformation applied to qubits from the one-qubit transformations and a certain two-qubit gate, such as the conditional sign-flip gate [2]. From these reasons, many physicists aim for realizing the two-qubit gate.

Here we show how to construct the conditional sign-flip gate with Jaynes-Cummings model (JCM), which is a quantum mechanical model describing the interaction between a single two-level atom and a single electromagnetic field mode. We also give discussions about experimental setups for realizing our scheme.

Properties of the JCM have been studied theoretically from 1960s [3, 4, 5, 6, 7] and they were confirmed by experiments in 1980s [8], so that the JCM is very familiar and well-studied to the researchers in the field of atomic and optical physics. Furthermore, these days, the JCM is used for describing the evolution of entanglement between the atom and the photons by the researchers of the quantum information science [9, 10]. (Azuma investigates the thermal JCM and discusses the lower bound of entanglement between the two-level atom and thermal photons [11].) Recently, so-called sudden death effect (disappearance of entanglement of two isolated Jaynes-Cummings atoms in a finite time) has been studied eagerly [12, 13, 14]. This phenomenon is experimentally demonstrated [15]. Thus, we can expect that our proposal grows to be one of the various applications of the JCM. Moreover, we can expect that our proposal becomes one of the important candidates for the method of implementing quantum logic, for example, cold trapped ions interacting with laser beams [16, 17], polarized photons in the cavity quantum electrodynamics system [18], and so on.

To construct a quantum computer, we have to prepare qubits and quantum logic gates. In our method, we regard a pair of optical paths where a photon is running as a qubit. (This construction of a qubit is called the dual-rail qubit representation [19].) We can apply any one-qubit transformation to this dual-rail qubit with beam splitters and phase shifters.

Knill, Laflamme, and Milburn (KLM) show a unique method for applying the conditional sign-flip gate to two dual-rail qubits using beam splitters and the nonlinear sign-shift (NS) gate [20], which causes the following transformation to the number states of photons:

$$\alpha|0\rangle_P + \beta|1\rangle_P + \gamma|2\rangle_P \rightarrow \alpha|0\rangle_P + \beta|1\rangle_P - \gamma|2\rangle_P. \quad (1)$$

(The index P stands for the photons.)

In this paper, we show the method for implementing the NS gate with the JCM. In KLM's proposal, the NS gate is constructed only with passive linear optics, and it works as a nondeterministic gate conditioned on the detection of an auxiliary photon.

Someone may make an objection to our proposal because we are going to introduce a nonlinear device into KLM's scheme. However, in our method, the NS gate works with small error probability in principle and the author thinks that our method is a practical compromise for the simplification of the whole system. (Gilchrist *et al.* try to build the NS gate by trapped atoms in an optical cavity [21]. Marchioli *et al.* investigate the JCM with an external field and give qualitative analyses about the entanglement between the atom and the cavity field [22, 23]. These studies seem to relate to our scheme. Azuma proposes a method for constructing the NS gate with one-dimensional Kerr-nonlinear photonic crystals [24]. This work aims to implement the NS gate with simple structures of matters. This work and our scheme explained in this paper share an idea of building the NS gate with a practical compromising method.)

This paper is organized as follows. In section 2, we explain how to build the NS gate by the JCM. In section 3, we discuss an experimental setup in which we make use of coherent lights to examine whether or not our scheme works. In section 4, we discuss an experimental setup in which an optical loop circuit made out of a polarizing beam splitter and the Pockels cell takes an important role in the cavity. In section 5, we explain the dual-rail qubit representation and KLM's scheme. In section 6, we give brief discussions.

2. Construction of the NS gate with the JCM

The JCM is originally designed for a spontaneous emission of the atom, and its Hamiltonian is given by $H = \hbar(C_1 + C_2)$, $C_1 = \omega[(1/2)\sigma_z + a^\dagger a]$, $C_2 = \kappa(\sigma_+ a + \sigma_- a^\dagger)$, where $\sigma_\pm = (1/2)(\sigma_x \pm i\sigma_y)$ and $[a, a^\dagger] = 1$. The Pauli matrices (σ_i , $i = x, y, z$) are operators of the atom, and a and a^\dagger are an annihilation and a creation operators of the electromagnetic field, respectively. Here, we assume that κ is a real constant and the field is resonant with the atom. (The photons' frequency is equal to the energy gap of the two-level atom.)

Because $[C_1, C_2] = 0$ and C_1 can be diagonalized at ease, we take the following interaction picture. We write a state vector of the whole system in the Schrödinger picture as $|\psi_S(t)\rangle$. A state vector in the interaction picture is defined by $|\psi_I(t)\rangle = \exp(iC_1 t)|\psi_S(t)\rangle$. [We assume $|\psi_I(0)\rangle = |\psi_S(0)\rangle$.] The time evolution of $|\psi_I(t)\rangle$ is given by $|\psi_I(t)\rangle = U(t)|\psi_I(0)\rangle$, where $U(t) = \exp(-iC_2 t)$.

We define the basis vectors for the state of the atom and the photons as follows. The ground and excited states of the atom are given by two-component vectors,

$$|g\rangle_A = \begin{pmatrix} 0 \\ 1 \end{pmatrix}, \quad |e\rangle_A = \begin{pmatrix} 1 \\ 0 \end{pmatrix}, \quad (2)$$

where we assume that $|g\rangle_A$ and $|e\rangle_A$ are eigenvectors of σ_z with eigenvalues -1 and 1 , respectively. (The index A stands for the atom.) The number states of the photons are described as $|n\rangle_P$ ($n = 0, 1, 2, \dots$).

Describing the atom's Pauli operators by 2×2 matrices, we can write down $U(t)$ as follows:

$$U(t) = \exp[-it \begin{pmatrix} 0 & \kappa a \\ \kappa a^\dagger & 0 \end{pmatrix}] = \begin{pmatrix} u_{00} & u_{01} \\ u_{10} & u_{11} \end{pmatrix}, \quad (3)$$

where

$$u_{00} = \cos(|\kappa|\sqrt{a^\dagger a + 1}t),$$

m	$ c(m) ^2$	$d(m)$
0	0.633	-0.606
1	0.138	0.928
2	0.988	0.111
3	0.024 7	-0.988
4	0.828	0.414

Table 1. The variation of the error probability $|c(m)|^2$ and the coefficient of $|g\rangle_A|1\rangle_P$ of the evolved state $d(m)$.

$$\begin{aligned}
u_{01} &= i\kappa a \frac{\sin(|\kappa|\sqrt{a^\dagger a}t)}{|\kappa|\sqrt{a^\dagger a}}, \\
u_{10} &= i\kappa a^\dagger \frac{\sin(|\kappa|\sqrt{a^\dagger a + 1}t)}{|\kappa|\sqrt{a^\dagger a + 1}}, \\
u_{11} &= \cos(|\kappa|\sqrt{a^\dagger a}t).
\end{aligned} \tag{4}$$

The time evolution of the three initial states, $|\psi_I(0)\rangle = |g\rangle_A|0\rangle_P$, $|g\rangle_A|1\rangle_P$, and $|g\rangle_A|2\rangle_P$ are given by

$$\begin{aligned}
U(t)|g\rangle_A|0\rangle_P &= U(t) \begin{pmatrix} 0 \\ |0\rangle_P \end{pmatrix} = \begin{pmatrix} 0 \\ |0\rangle_P \end{pmatrix}, \\
U(t)|g\rangle_A|1\rangle_P &= U(t) \begin{pmatrix} 0 \\ |1\rangle_P \end{pmatrix} = \begin{pmatrix} i(\kappa/|\kappa|)\sin(|\kappa|t)|0\rangle_P \\ \cos(|\kappa|t)|1\rangle_P \end{pmatrix}, \\
U(t)|g\rangle_A|2\rangle_P &= U(t) \begin{pmatrix} 0 \\ |2\rangle_P \end{pmatrix} = \begin{pmatrix} i(\kappa/|\kappa|)\sin(\sqrt{2}|\kappa|t)|1\rangle_P \\ \cos(\sqrt{2}|\kappa|t)|2\rangle_P \end{pmatrix}.
\end{aligned} \tag{5}$$

We want to obtain the NS gate, which flips only the sign of the coefficient of $|2\rangle_P$. Thus, we let $t = (2m+1)\pi/(\sqrt{2}|\kappa|)$ for $m = 0, 1, 2, \dots$, and we obtain the following time evolution: $|g\rangle_A|0\rangle_P \rightarrow |g\rangle_A|0\rangle_P$, $|g\rangle_A|1\rangle_P \rightarrow c(m)|e\rangle_A|0\rangle_P + d(m)|g\rangle_A|1\rangle_P$, $|g\rangle_A|2\rangle_P \rightarrow -|g\rangle_A|2\rangle_P$, where $c(m) = i(\kappa/|\kappa|)\sin[(2m+1)\pi/\sqrt{2}]$ and $d(m) = \cos[(2m+1)\pi/\sqrt{2}]$.

In table 1, we show values of $|c(m)|^2$ and $d(m)$ for $m = 0, 1, 2, 3, 4$. We pay attention to the cases of $m = 1$ and $m = 3$. When we let $m = 1$, $|c(1)|^2$ takes a small value and $d(1)$ is nearly equal to one. This implies that if we let $t = 3\pi/(\sqrt{2}|\kappa|)$, we obtain the operation of the NS gate shown in (1) with the error probability upper bound 0.138. When we let $m = 3$, $|c(3)|^2$ is nearly equal to zero and $d(m)$ is nearly equal to -1 . This implies that if we let $t = 7\pi/(\sqrt{2}|\kappa|)$, we obtain the transformation, $\alpha|0\rangle_P + \beta|1\rangle_P + \gamma|2\rangle_P \rightarrow \alpha|0\rangle_P - \beta|1\rangle_P - \gamma|2\rangle_P$ with the error probability upper bound 0.024 7. To flip the sign of the coefficient of $|1\rangle_P$ after this transformation, we apply a phase shifter to the photons. This device causes the operation, $|n\rangle_P \rightarrow (-1)^n|n\rangle_P$, so that we obtain the transformation, $\alpha|0\rangle_P - \beta|1\rangle_P - \gamma|2\rangle_P \rightarrow \alpha|0\rangle_P + \beta|1\rangle_P - \gamma|2\rangle_P$, and we finally obtain the transformation of the NS gate shown in (1) with the error probability upper bound 0.024 7.

3. An experimental setup for examining the function of the NS gate using coherent lights

In our scheme explained in section 2, we have to put the photons' initial state, $\alpha|0\rangle_P + \beta|1\rangle_P + \gamma|2\rangle_P$, into the cavity and let it develop into the cavity mode. Then, we

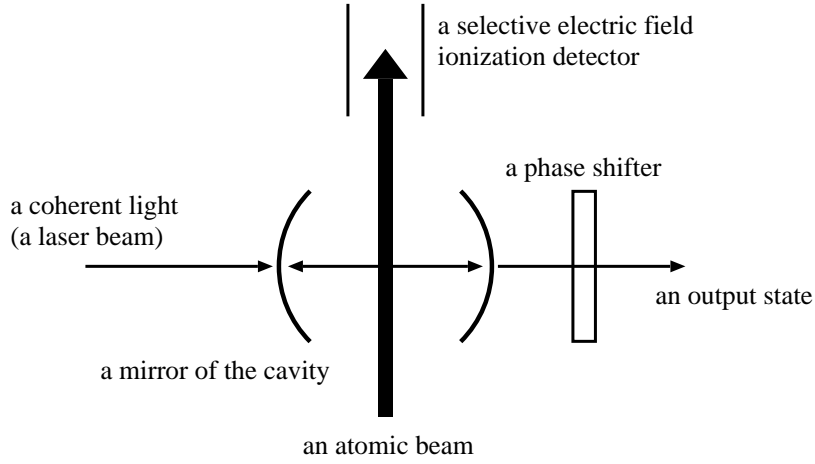


Figure 1. An outline of the experimental setup which examines whether or not the NS gate realized by our scheme works. A coherent light (a laser beam) is fed to the cavity from its left side and reflected by mirrors of the cavity many times, so that it becomes a cavity field. The two-level atom passes the cavity as a slow beam and it causes the Jaynes-Cummings interaction with the cavity field. Then, the time-evolved state of the cavity field runs away from the cavity to its right side. [Strictly speaking, the time-evolved state of the cavity field can fly away from the cavity to its either side (the right side and the left side). However, to let the discussion be simple, we assume that the time-evolved light goes outside of the cavity from its right side in this figure.] If the time of flight of the atom through the cavity is given by $T = 3\pi/(\sqrt{2}|\kappa|)$, we need not put a phase shifter behind the cavity. In contrast, if $T = 7\pi/(\sqrt{2}|\kappa|)$, we have to put it there. A selective electric field ionization detector distinguishes the atom's ground state $|g\rangle_A$ from its excited state $|e\rangle_A$, so that we can examine whether the NS gate works or fails. The output state of the NS gate is sent to the path $a1$ of the beam splitter BS1 in figure 2.

have to let the cavity mode interact with the two-level atom as the JCM, and finally extract the evolved state of photons from the cavity. In general, it is very difficult to perform these sequential procedures actually in the laboratory.

In this section, we give an experimental setup in which we make use of coherent lights to examine whether or not our scheme works. An outline of the experimental setup is shown in figures 1 and 2.

In figure 2, symbols BS1 and BS2 represent beam splitters (half-silvered mirrors), which transform the incident number states of paths $a1$ and $a2$ as follows:

$$\begin{aligned}
 |n\rangle_{a1}|m\rangle_{a2} &= \frac{1}{\sqrt{n!m!}}(a_1^\dagger)^n(a_2^\dagger)^m|0\rangle_{a1}|0\rangle_{a2} \\
 &\rightarrow \frac{1}{\sqrt{n!m!}}\left[\frac{1}{\sqrt{2}}(a_1^\dagger + a_2^\dagger)\right]^n\left[\frac{1}{\sqrt{2}}(a_1^\dagger - a_2^\dagger)\right]^m|0\rangle_{a1}|0\rangle_{a2} \\
 &\quad \text{for } n, m \in \{0, 1, 2, \dots\},
 \end{aligned} \tag{6}$$

where a_1^\dagger and a_2^\dagger are creation operators of photons on the paths $a1$ and $a2$, respectively. A symbol PS- θ represent a phase shifter which causes the operation, $|n\rangle_P \rightarrow e^{in\theta}|n\rangle_P$, where $|n\rangle_P$ is the number state of the photons. Symbols D1 and D2 represent detectors which count the number of incident photons, so that D1 and D2 identify differences in the number states of the photons, $|0\rangle_P, |1\rangle_P, |2\rangle_P, \dots$.

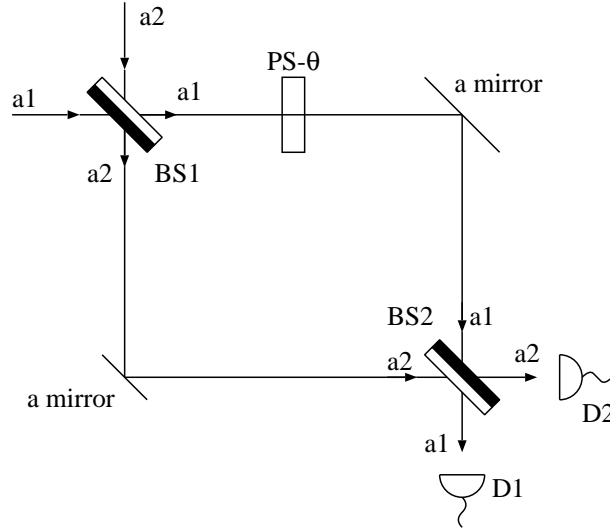


Figure 2. The Mach-Zehnder interferometer that examine the output state of the NS gate outlined in figure 1. Symbols BS1 and BS2 represent beam splitters (half-silvered mirrors). A symbol PS- θ represent a phase shifter which causes the operation, $|n\rangle_{\text{P}} \rightarrow e^{in\theta}|n\rangle_{\text{P}}$, where $|n\rangle_{\text{P}}$ is the number state of the photons. Symbols D1 and D2 represent detectors which count the number of incident photons. The output state of the NS gate in figure 1 is injected to the beam splitter BS1 through the path a1. At the same time, we inject another coherent light into the path a2 of the beam splitter BS1 to let it interfere with the output state of the NS gate in figure 1.

The experimental setup shown in figure 1 works as follows. First, we feed a strong laser beam (a coherent light) to the cavity from its left side. Although the transmittance of the mirror of the cavity is quite low, a few photons pass the mirror and they are reflected by the mirrors of both sides of the cavity many times. After this process, the photons in the cavity develop into a coherent light of the cavity mode, which is given by

$$\begin{aligned}
 |\alpha\rangle &= \exp(-|\alpha|^2/2) \sum_{n=0}^{\infty} \frac{\alpha^n}{\sqrt{n!}} |n\rangle_{\text{P}} \\
 &= \exp(-|\alpha|^2/2) \sum_{n=0}^{\infty} \frac{(\alpha a^\dagger)^n}{n!} |0\rangle_{\text{P}} \\
 &= \exp(-|\alpha|^2/2) e^{\alpha a^\dagger} |0\rangle_{\text{P}}, \tag{7}
 \end{aligned}$$

where α is an arbitrary complex number. (In the notation of the coherent states of photons, we omit the index P.) We can assume that this coherent light is weak, so that $|\alpha| < 1$. We let the width of the cavity (the length between the mirrors of the cavity) be equal to a half of the wavelength of the coherent light. Thus, the cavity mode forms a standing wave.

Second, we put the two-level atom at an anti-node of the standing wave of the cavity mode. For example, we can capture and locate an ionized atom in a certain region by a technique of the Paul trap (a quadrupole ion trap) [25]. We can also locate the atom in a certain area by injecting a slow atomic beam there. Then, the

coherent light $|\alpha\rangle$ interacts with the atom as the JCM. If the time of flight of the atom is equal to $T = 3\pi/(\sqrt{2}|\kappa|)$ or $T = 7\pi/(\sqrt{2}|\kappa|)$, and if we observe $|g\rangle_A$ with the selective electric field detector in figure 1, an approximate NS gate is realized. The coherent state $|\alpha\rangle$ is transformed and the reduction of the state vector is occurred as follows:

$$\begin{aligned}
|\alpha\rangle &= \exp(-|\alpha|^2/2)(|0\rangle_P + \alpha|1\rangle_P + \frac{\alpha^2}{\sqrt{2}}|2\rangle_P) + O(|\alpha|^3)|\varphi^{(1)}\rangle_P \\
\longrightarrow |\Psi\rangle_P &= \text{Const.} \exp(-|\alpha|^2/2)[|0\rangle_P + d(m)\alpha|1\rangle_P - \frac{\alpha^2}{\sqrt{2}}|2\rangle_P] \\
&\quad + O(|\alpha|^3)|\varphi^{(2)}\rangle_P \\
&= |0\rangle_P + d(m)\alpha|1\rangle_P - \frac{\alpha^2}{\sqrt{2}}|2\rangle_P \\
&\quad + O(|\alpha|^2)|0\rangle_P + O(|\alpha|^3)|1\rangle_P + O(|\alpha|^4)|2\rangle_P \\
&\quad + O(|\alpha|^3)|\varphi^{(3)}\rangle_P, \tag{8}
\end{aligned}$$

where $|\varphi^{(1)}\rangle_P$, $|\varphi^{(2)}\rangle_P$, and $|\varphi^{(3)}\rangle_P$ are superpositions of $\{|3\rangle_P, |4\rangle_P, |5\rangle_P, \dots\}$, $m = 1$ or 3, and Const. is the normalization constant.

Here, we define the following superposition of two coherent states:

$$\begin{aligned}
&\frac{1}{2}(|e^{i\pi/3}\alpha\rangle + |e^{-i\pi/3}\alpha\rangle) \\
&= \exp(-|\alpha|^2/2)(|0\rangle_P + \alpha|1\rangle_P - \frac{\alpha^2}{\sqrt{2}}|2\rangle_P) + O(|\alpha|^3)|\varphi^{(4)}\rangle_P, \tag{9}
\end{aligned}$$

where $|\varphi^{(4)}\rangle_P$ is a superposition of $\{|3\rangle_P, |4\rangle_P, |5\rangle_P, \dots\}$. Then, we obtain the following relation:

$$1 - \frac{1}{4}|(\langle e^{i\pi/3}\alpha| + \langle e^{-i\pi/3}\alpha|)|\Psi\rangle_P|^2 = O(|\alpha|^2). \tag{10}$$

Thus, we can regard the output state of the cavity shown in figure 1 as $(1/2)(|e^{i\pi/3}\alpha\rangle + |e^{-i\pi/3}\alpha\rangle)$ with the error probability $O(|\alpha|^2)$.

Finally, we have to extract the time-evolved state of the cavity field from the cavity. Although the transmittance of the mirror of the cavity is quite low, the time-evolved photons can go outside the cavity gradually over a long period of time. [Strictly speaking, the time-evolved state of the cavity field can fly away from the cavity to its either side (the right side and the left side). However, to let the discussion be simple, we assume that the time-evolved light goes outside of the cavity from its right side in figure 1.]

Next, we examine the output state of the NS gate outlined in figure 1 with the Mach-Zehnder interferometer shown in figure 2. The interferometer of figure 2 works as follows. First, we inject the output state generated by the NS gate in figure 1 into the path $a1$ of the beam splitter BS1. At the same time, we inject another coherent light $|\alpha\rangle_{a2}$ into the path $a2$ of BS1 to let it interfere with the output state of the NS gate in figure 1. Second, we apply the phase shifter PS- θ to the state of path $a1$. Third, we apply beam splitter BS2 to the paths $a1$ and $a2$. Finally, we count the number of photons on each path, $a1$ and $a2$, by the detectors D1 and D2, respectively.

Here, we follow the transformations applied to states of incident photons in this interferometer. Before discussing the function of the interferometer in figure 2 in detail, we consider two coherent lights $|\alpha\rangle$ and $|\beta\rangle$ injected into the paths $a1$ and $a2$ of the beam splitter BS1, respectively. Remembering the operation of BS1 in (6) and

the definition of the coherent light in (7), we can describe the transformation caused by the beam splitter BS1 as follows:

$$\begin{aligned}
|\alpha\rangle_{a1}|\beta\rangle_{a2} &= \exp[-(|\alpha|^2 + |\beta|^2)/2] \\
&\quad \times \exp(\alpha a_1^\dagger) \exp(\beta a_2^\dagger) |0\rangle_{a1} |0\rangle_{a2} \\
&\xrightarrow{\text{BS1}} \exp[-(|\alpha|^2 + |\beta|^2)/2] \\
&\quad \times \exp\left[\frac{\alpha}{\sqrt{2}}(a_1^\dagger + a_2^\dagger)\right] \exp\left[\frac{\alpha}{\sqrt{2}}(a_1^\dagger - a_2^\dagger)\right] |0\rangle_{a1} |0\rangle_{a2} \\
&= \exp[-(|\alpha|^2 + |\beta|^2)/2] \exp\left[\frac{1}{\sqrt{2}}(\alpha + \beta)a_1^\dagger\right] |0\rangle_{a1} \\
&\quad \otimes \exp\left[\frac{1}{\sqrt{2}}(\alpha - \beta)a_2^\dagger\right] |0\rangle_{a2} \\
&= \left|\frac{1}{\sqrt{2}}(\alpha + \beta)\right\rangle_{a1} \left|\frac{1}{\sqrt{2}}(\alpha - \beta)\right\rangle_{a2}. \tag{11}
\end{aligned}$$

Moreover, we think about how the phase shifter PS- θ works against the coherent light,

$$\begin{aligned}
|\alpha\rangle &\xrightarrow{\text{PS-}\theta} \exp(-|\alpha|^2/2) \sum_{n=0}^{\infty} \frac{(\alpha e^{i\theta})^n}{\sqrt{n!}} |n\rangle_P \\
&= |e^{i\theta}\alpha\rangle. \tag{12}
\end{aligned}$$

From the above formulas, we can describe the transformation applied to coherent states in the interferometer as follows:

$$\begin{aligned}
&|\alpha\rangle_{a1}|\beta\rangle_{a2} \\
&\xrightarrow{\text{BS1}} \left|\frac{1}{\sqrt{2}}(\alpha + \beta)\right\rangle_{a1} \left|\frac{1}{\sqrt{2}}(\alpha - \beta)\right\rangle_{a2} \\
&\xrightarrow{\text{PS-}\theta} \left|\frac{e^{i\theta}}{\sqrt{2}}(\alpha + \beta)\right\rangle_{a1} \left|\frac{1}{\sqrt{2}}(\alpha - \beta)\right\rangle_{a2} \\
&\xrightarrow{\text{BS2}} \left|\frac{1}{2}[(e^{i\theta} + 1)\alpha + (e^{i\theta} - 1)\beta]\right\rangle_{a1} \\
&\quad \otimes \left|\frac{1}{2}[(e^{i\theta} - 1)\alpha + (e^{i\theta} + 1)\beta]\right\rangle_{a2}. \tag{13}
\end{aligned}$$

Hence, the Mach-Zehnder interferometer in figure 2 performs the transformation against the output state of the cavity in (9) as follows:

$$\begin{aligned}
&\frac{1}{2}(|e^{i\pi/3}\alpha\rangle_{a1} + |e^{-i\pi/3}\alpha\rangle_{a1})|\alpha\rangle_{a2} + O(|\alpha|^2) \\
&\longrightarrow \frac{1}{2}\left|\frac{1}{2}\alpha F_1(\theta)\right\rangle_{a1} \left|\frac{1}{2}\alpha F_2(\theta)\right\rangle_{a2} \\
&\quad + \frac{1}{2}\left|\frac{1}{2}\alpha F_3(\theta)\right\rangle_{a1} \left|\frac{1}{2}\alpha F_4(\theta)\right\rangle_{a2} + O(|\alpha|^2), \tag{14}
\end{aligned}$$

where

$$\begin{aligned}
F_1(\theta) &= (e^{i\theta} + 1)e^{i\pi/3} + (e^{i\theta} - 1), \\
F_2(\theta) &= (e^{i\theta} - 1)e^{i\pi/3} + (e^{i\theta} + 1), \\
F_3(\theta) &= (e^{i\theta} + 1)e^{-i\pi/3} + (e^{i\theta} - 1), \\
F_4(\theta) &= (e^{i\theta} - 1)e^{-i\pi/3} + (e^{i\theta} + 1). \tag{15}
\end{aligned}$$

[In (14), the term of $O(|\alpha|^2)$ implies the error probability.]

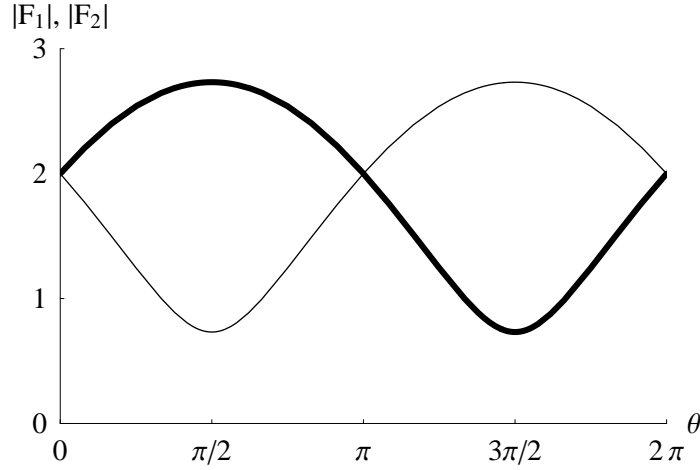


Figure 3. Graphs of $|F_1(\theta)|$ and $|F_2(\theta)|$ for $\theta \in [0, 2\pi]$. A thick curve represents $|F_1(\theta)|$ and a thin curve represents $|F_2(\theta)|$. Seeing these graphs, we notice the following facts. When $\theta = \pi/2$, $|F_1(\theta)|$ reaches the maximum value as $|F_1(\pi/2)| = 2.732$ and $|F_2(\theta)|$ reaches the minimum value as $|F_2(\pi/2)| = 0.7321$.

We can obtain the following relation,

$$|F_1(\theta)| = |F_4(\theta)|, \quad |F_2(\theta)| = |F_3(\theta)| \quad \forall \theta. \quad (16)$$

We plot $|F_1(\theta)|$ and $|F_2(\theta)|$ for $\theta \in [0, 2\pi]$ in figure 3. Seeing figure 3, we notice the following facts. When $\theta = \pi/2$, $|F_1(\theta)|$ and $|F_4(\theta)|$ reach the maximum value as $|F_1(\pi/2)| = |F_4(\pi/2)| = 2.732$ and $|F_2(\theta)|$ and $|F_3(\theta)|$ reach the minimum value as $|F_2(\pi/2)| = |F_3(\pi/2)| = 0.7321$.

The right-hand side of (14) shows a sign of weak entanglement between paths $a1$ and $a2$. (This weak entanglement is generated by the photon bunching.) Thus, if we repeat the experiment in figures 1 and 2 many times and store the statistical data observed with the detectors D1 and D2, we can obtain some information about the function of the cavity shown in figure 1.

Here, for example, we assume $\alpha = 0.5$ and $\theta = \pi/2$. We obtain $|(1/2)\alpha F_1(\theta)|^2 = |(1/2)\alpha F_4(\theta)|^2 = 0.4665$ and $|(1/2)\alpha F_2(\theta)|^2 = |(1/2)\alpha F_3(\theta)|^2 = 0.03349$. In this case, the error probability $O(|\alpha|^2)$ is given by 0.25 around. If we perform photon counting against $|(1/2)\alpha F_1(\theta)\rangle_{a1}$ or $|(1/2)\alpha F_4(\theta)\rangle_{a2}$, we obtain the Poisson distribution whose mean is given by $|(1/2)\alpha F_1(\theta)|^2 = |(1/2)\alpha F_4(\theta)|^2 = 0.4665$. If we perform photon counting against $|(1/2)\alpha F_2(\theta)\rangle_{a2}$ or $|(1/2)\alpha F_3(\theta)\rangle_{a1}$, we obtain the Poisson distribution whose mean is given by $|(1/2)\alpha F_2(\theta)|^2 = |(1/2)\alpha F_3(\theta)|^2 = 0.03349$. We plot these distribution functions in figure 4.

If we detect one photon by the detector D2, we become aware of reduction of the state vector on the path $a1$ to $|(1/2)\alpha F_3(\theta)\rangle_{a1}$ with a comparatively high probability. [We describe the Poisson distribution with a mean μ as

$$P(n, \mu) = e^{-\mu} \frac{\mu^n}{n!} \quad \text{for } n = 0, 1, 2, \dots \quad (17)$$

Because $P(1, 0.4665) = 0.2926$, $P(1, 0.03349) = 0.03239$, and $P(1, 0.4665) > P(1, 0.03349)$, we can expect that this reduction of the state vector occurs with comparatively high probability.]

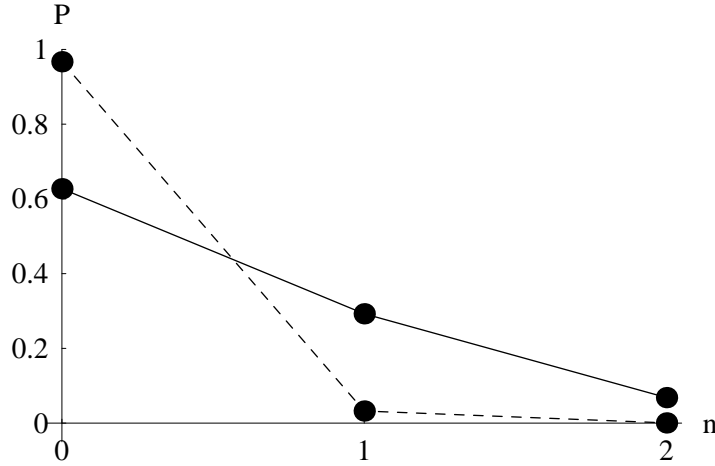


Figure 4. Graphs of the Poisson distribution functions, $P(n, \mu) = e^{-\mu} \mu^n / n!$ for $n = 0, 1, 2$ with $\mu = 0.4665$ and $\mu = 0.03349$. (The variable μ represents a mean.) A solid line represents $P(n, 0.4665)$ and a broken line represents $P(n, 0.03349)$. We note that $P(1, 0.4665) = 0.2926$ and $P(1, 0.03349) = 0.03239$. We also note that $P(2, 0.4665) = 0.06825$ and $P(2, 0.03349) = 0.0005424$.

In this case, the probability that the detector D2 observes one photon is given by $0.2926/4 = 0.07315$ around. This probability seems to be smaller than the error probability $O(|\alpha|^2) \sim 0.25$, so that we need careful data analysis. However, anyway, repeating the experiment many times and storing the statistical data which is a set of events conditioned on the detection of $|1\rangle_{a2}$ by the detector D2, we obtain the Poisson distribution that comes from the coherent state $|(1/2)\alpha F_3(\theta)\rangle_{a1}$ with the error probability $O(|\alpha|^2)$. [Because $|(1/2)\alpha F_3(\theta)|^2 = 0.03349$ is much smaller than unity, we have to store huge amounts of data of experiments for detecting $|(1/2)\alpha F_3(\theta)\rangle_{a1}$.]

Hence, we can examine whether or not the NS gate realized in figure 1 works with the interferometer shown in figure 2.

4. An experimental setup for constructing the NS gate using an optical loop circuit

In section 3, we discuss the NS gate which only accepts the coherent state as an input. However, to construct the genuine NS gate, we have to put an arbitrary superposition of $\{|0\rangle_P, |1\rangle_P, |2\rangle_P\}$ into the cavity, let it interact with the two-level atom, and extract the time-evolved state of the photons from the cavity. In this section, we try to show another experimental setup for carrying out these procedures. We make an optical loop circuit out of a polarizing beam splitter and the Pockels cell in the cavity and we let an arbitrary superposition of $\{|0\rangle_P, |1\rangle_P, |2\rangle_P\}$ develop into the cavity mode. In this method, for building the optical loop, the polarization degree of freedom of photons plays an important role. (Kwiat *et al.* construct an optical loop circuit from the polarizing beam splitters and the Pockels cells actually in their experiment [26].)

First, we introduce the polarization degree of freedom to photons. We describe photons' state vectors as follows: $\{|n\rangle_P|V\rangle_P, |n\rangle_P|H\rangle_P : n = 0, 1, 2, \dots\}$, where $|V\rangle_P$ and $|H\rangle_P$ imply the photons' vertical and horizontal polarization states, respectively.

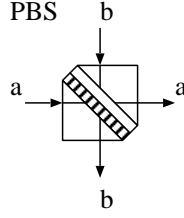


Figure 5. The polarizing beam splitter (PBS). It has two paths a and b .

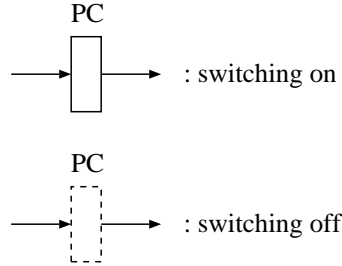


Figure 6. The Pockels cell (PC). It has only one path.

Second, we prepare two kinds of devices which apply unitary transformation to photons' polarization states: a polarizing beam splitter and the Pockels cell. (We let PBS and PC be the symbols of the polarizing beam splitter and the Pockels cell, respectively.)

We draw the PBS in figure 5. The PBS splits an unpolarized light into beams of differing polarization (two orthogonal linearly polarized states, that is, vertical and horizontal polarization states). For example, we can utilize the Wollaston prism as the PBS. Describing the PBS's incoming and outgoing paths a and b as states,

$$|a\rangle = \begin{pmatrix} 1 \\ 0 \end{pmatrix}, \quad |b\rangle = \begin{pmatrix} 0 \\ 1 \end{pmatrix}, \quad (18)$$

we can describe a unitary transformation that the PBS applies to polarized photons as

$$U_{\text{PBS}} = \begin{pmatrix} |V\rangle\langle V| & |H\rangle\langle H| \\ |H\rangle\langle H| & |V\rangle\langle V| \end{pmatrix}. \quad (19)$$

(From now on, to let the notation be simple, we omit the index P from $|V\rangle_P$ and $|H\rangle_P$.) For instance, if we inject $(c_V|V\rangle + c_H|H\rangle)$ into the PBS from the path a , $c_V|V\rangle$ and $c_H|H\rangle$ are separated and run away from the PBS through the paths a and b , respectively.

We draw the PC in figure 6. The PC is a voltage-controlled wave plate. If we apply the voltage to the PC (switching on), polarized photons' states injected into the PC are transformed as $|V\rangle \rightarrow |H\rangle$ and $|H\rangle \rightarrow |V\rangle$, and they run away from the PC. If we do not apply the voltage to the PC (switching off), the PC leaves injected polarized photons' states untouched and returns them as outputs.

Third, we construct an optical circuit in the cavity as shown in figures 7, 8, and 9. We inject the photons' wave function initialized as $|H\rangle$ into the PBS and it is reflected

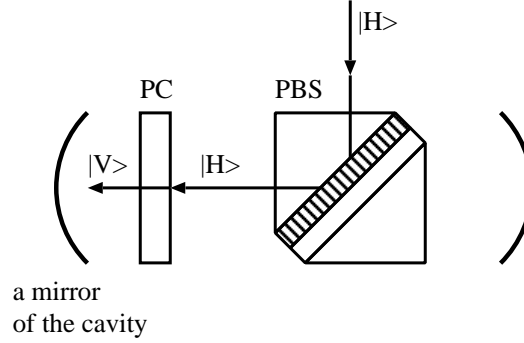


Figure 7. An optical circuit built in the cavity. In this case, the PC is switched on. The initially polarized photons $|H\rangle$ is put into PBS from its upper side, and the PBS reflects $|H\rangle$ to its left side. The PC transforms the incoming $|H\rangle$ into the outgoing $|V\rangle$. Then, the mirror on the left side of the cavity reflects $|V\rangle$.

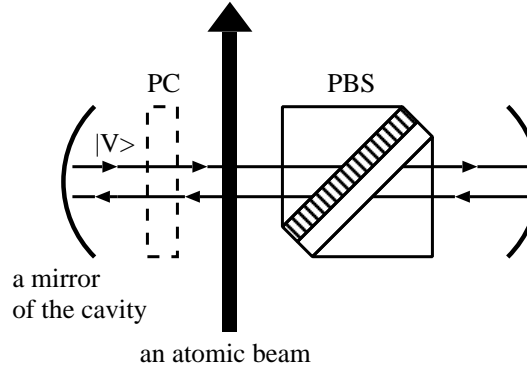


Figure 8. An optical circuit built in the cavity. In this case, the PC is switched off. Because the mirrors on the both sides of the cavity reflect $|V\rangle$, the optical circuit forms a closed loop. The photons polarized as $|V\rangle$ fly along the closed loop many times, and they become a cavity field. In the area where the atom is located, the cavity field causes the Jaynes-Cummings interaction with the atom.

by the PBS as shown in figure 7. At this moment, we switch on the PC, so that the photons' state $|H\rangle$ is transformed into $|V\rangle$. Then, $|V\rangle$ flies against the mirror of the cavity in the left side and it is reflected by the mirror. Next moment, we switch off the PC as shown in figure 8. Because the photons' state $|V\rangle$ passes across the PBS, it is reflected by the mirrors on the both sides of the cavity and it runs along an optical closed loop. While the photons in the state of $|V\rangle$ run along this loop many times, they develop into the cavity mode. This cavity mode causes the Jaynes-Cummings interaction with the two-level atom which is injected into the cavity as a slow atomic beam. After a period for constructing the NS gate $[T = 3\pi/(\sqrt{2}|\kappa|)$ or $7\pi/(\sqrt{2}|\kappa|)]$, we switch on the PC as shown in figure 9. Because the PC transforms the photons' state $|V\rangle$ reflected by the mirror on the left side of the cavity into $|H\rangle$, the photons are reflected by the PBS and they run away from the cavity.

The above is the outline for constructing the cavity mode with an optical circuit.

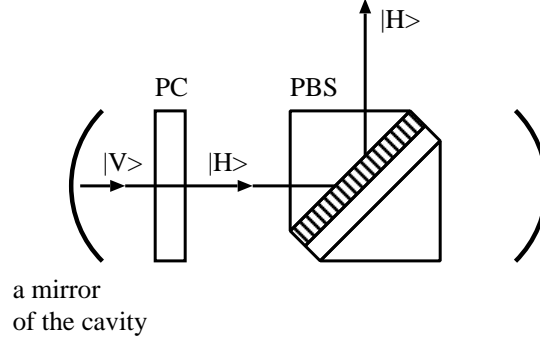


Figure 9. An optical circuit built in the cavity. In this case, the PC is switched on. After reflected by the mirror on the left side of the cavity, $|V\rangle$ flies against the PC and the PC transforms $|V\rangle$ into $|H\rangle$. And then, the polarized photons' state $|H\rangle$ is reflected by the PBS to its upper side, so that the photons run away from the cavity.

From the theoretical viewpoint, our optical circuit works in principle. However, examining each optical device in the circuit, we notice some problems for us to perform this experiment actually. Here, we try to go into details about each device.

To construct the closed loop, we have to turn on and off the Pockels cell a few times at short intervals. At the present time, the Pockels cell that has a 2.5×10^{-10} s time response has been developed. In the experiment of the JCM with the cavity quantum electrodynamics system carried by Rempe *et al.* [8], $63p_{3/2} \leftrightarrow 61d_{5/2}$ transition of ^{85}Rb ($f = 21\,456.0 \times 10^6$ Hz, $\lambda = 1.397\,24 \times 10^{-2}$ m) is made use of for the two-level atom, and their cavity gives the coupling constant $|\kappa| \simeq (1/70) \times 10^6$ s $^{-1}$. If we construct the optical loop circuit in the cavity whose width is given by $L = \lambda/2 = 6.986 \times 10^{-3}$ m, the time response required to the PC is estimated at $L/c = 2.330 \times 10^{-11}$ s, where $c = 2.998 \times 10^8$ ms $^{-1}$ is a velocity of the light. Thus, at present, we cannot prepare such a ultra-fast Pockels cell which is available in our experiment. If we construct the cavity whose coupling constant is similar to that in Rempe *et al.*'s experiment, the period of the time evolution for the JCM is estimated to be $T = 3\pi/(\sqrt{2}|\kappa|) \simeq 4.67 \times 10^{-4}$ s for $m = 1$ and $T = 7\pi/(\sqrt{2}|\kappa|) \simeq 1.09 \times 10^{-3}$ s for $m = 3$.

In figure 8, the photons pass across the PC and the PBS. At present, the rate of the insertion loss of the PC is given by 0.04 around. In contrast, the rate of the insertion loss of the PBS is lower than 0.01. Thus, in our optical loop, cavity loss due to dissipative effect in the Pockels cell is very serious.

Finally, we have to point out a fact that to make a small optical circuit in the cavity is difficult even with the latest technology. If we build the optical circuit in the cavity, its size may be around a few centimeters. (The size of available optical devices on the market is around a few centimeters.) The coupling constant $|\kappa|$ is proportional to $\sqrt{\omega/L^3}$, where L^3 is the volume of the cavity. Hence, to make a small cavity is favourable to us. In Rempe *et al.*'s experimental setup, photon's wavelength is given by $\lambda = 1.397\,24 \times 10^{-2}$ m ($f = 21\,456.0 \times 10^6$ Hz) [8]. Thus, the length between mirrors in the cavity has to be equal to $\lambda/2 = 6.986 \times 10^{-3}$ m.

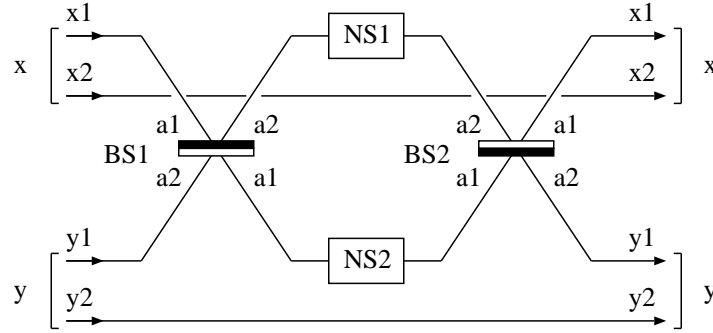


Figure 10. Implementation of the conditional sign-flip gate with the NS operations. Qubits x and y consist of a pair of paths $x1$ and $x2$ and a pair of paths $y1$ and $y2$, respectively. Symbols BS1 and BS2 represent beam splitters (half-silvered mirrors). Symbols NS1 and NS2 represent the NS gates. Photons travel from left to right in this network.

5. Dual-rail qubits and KLM's scheme

In this section, we explain the dual-rail qubit representation and KLM's scheme. To build a qubit, we prepare a pair of optical paths, $x1$ and $x2$. The optical path forms a system which takes a superposition of the number states $|n\rangle_P$ for $n = 0, 1, 2, \dots$, where n is the number of photons on the path. $|0\rangle_{x1} \otimes |1\rangle_{x2}$ is a state where paths $x1$ and $x2$ have zero and one photons, respectively, and we regard it as a logical ket vector $|\bar{0}\rangle_x$. We regard $|1\rangle_{x1} \otimes |0\rangle_{x2}$ as a logical ket vector $|\bar{1}\rangle_x$, similarly. And we describe an arbitrary state of a qubit as $|\phi\rangle_x = \alpha|\bar{0}\rangle_x + \beta|\bar{1}\rangle_x$.

An optical network drawn in figure 10 works as the conditional sign-flip gate, whose operation is given by $|\bar{j}\rangle_x \otimes |\bar{k}\rangle_y \rightarrow (-1)^{jk}|\bar{j}\rangle_x \otimes |\bar{k}\rangle_y$ for $j, k \in \{0, 1\}$. Here, we confirm the function of this network. In figure 10, symbols BS1 and BS2 represent beam splitters (half-silvered mirrors), which transform the incident number states of paths $a1$ and $a2$ as (6). We give attention to the fact that BS2 applies an inverse transformation of BS1. Symbols NS1 and NS2 represent the NS gates.

If we put a superposition of $|\bar{0}\rangle_x|\bar{0}\rangle_y$, $|\bar{0}\rangle_x|\bar{1}\rangle_y$, and $|\bar{1}\rangle_x|\bar{0}\rangle_y$ into the left side of the network shown in figure 10, the network leaves it untouched and returns it as an output from the right side of the network. However, if we put a state $|\bar{1}\rangle_x|\bar{1}\rangle_y = |1\rangle_{x1}|0\rangle_{x2}|1\rangle_{y1}|0\rangle_{y2}$ into the network, the following transformation is applied to the paths $x1$ and $y1$:

$$\begin{aligned}
|1\rangle_{x1}|1\rangle_{y1} &\xrightarrow{\text{BS1}} \frac{1}{\sqrt{2}}(|2\rangle_{a1}|0\rangle_{a2} - |0\rangle_{a1}|2\rangle_{a2}) \\
&\xrightarrow{\text{NS1,NS2}} -\frac{1}{\sqrt{2}}(|2\rangle_{a1}|0\rangle_{a2} - |0\rangle_{a1}|2\rangle_{a2}) \\
&\xrightarrow{\text{BS2}} -|1\rangle_{x1}|1\rangle_{y1}.
\end{aligned} \tag{20}$$

Thus, we obtain $-|\bar{1}\rangle_x|\bar{1}\rangle_y = -|1\rangle_{x1}|0\rangle_{x2}|1\rangle_{y1}|0\rangle_{y2}$ as an output for the input state $|\bar{1}\rangle_x|\bar{1}\rangle_y$. Hence, we confirm that the network shown in figure 10 realizes the conditional sign-flip gate.

6. Discussions

In this paper, we discuss how to build Knill, Laflamme, and Milburn's nonlinear sign-shift gate with the Jaynes-Cummings model. We also discuss the experimental setups for our scheme. The first one of our experimental setups seems to be practical and easy to carry out in the laboratory because it utilizes coherent lights. In contrast, the second one of our experimental setups seems to be difficult to demonstrate actually because it requires optical devices that have very excellent performance. However, because optical devices' performance is improving rapidly, the author thinks that our second experimental setup will be demonstrated in the near future.

As we mentioned in section 1, although the Jaynes-Cummings model was born about forty years ago, it is studied from the new viewpoint by the researchers of the quantum information theory [9, 10, 12, 13, 14, 15, 21, 22, 23]. The author thinks that we can find many new applications from the Jaynes-Cummings model.

Acknowledgments

The author thanks K. Kuwahara and colleagues of iCFD for encouragement. The author also thanks W. J. Munro and M. A. Marchioli for drawing his attention to references [21, 22, 23].

- [1] Shor P W 1997 *SIAM J. Comput.* **26** 1484–509
- [2] Barenco A, Bennett C H, Cleve R, DiVincenzo D P, Margolus N, Shor P, Sleator T, Smolin J A and Weinfurter H 1995 *Phys. Rev. A* **52** 3457–67
- [3] Jaynes E T and Cummings F W 1963 *Proc. IEEE* **51** 89–109
- [4] Shore B W and Knight P L 1993 *J. Mod. Opt.* **40** 1195–238
- [5] Louisell W H 1973 *Quantum Statistical Properties of Radiation* (New York: Wiley) section 5.13
- [6] Walls D F and Milburn G J 1994 *Quantum Optics* (Berlin: Springer-Verlag) chapter 10
- [7] Schleich W P 2001 *Quantum Optics in Phase Space* (Berlin: Wiley-VCH) chapter 15
- [8] Rempe G, Walther H and Klein N 1987 *Phys. Rev. Lett.* **58** 353–6
- [9] Bose S, Fuentes-Guridi I, Knight P L and Vedral V 2001 *Phys. Rev. Lett.* **87** 050401; 2001 *Phys. Rev. Lett.* **87** 279901(E)
- [10] Scheel S, Eisert J, Knight P L and Plenio M B 2003 *J. Mod. Opt.* **50** 881–9
- [11] Azuma H 2008 *J. Phys. D: Appl. Phys.* **41** 025102
- [12] Yu T and Eberly J H 2004 *Phys. Rev. Lett.* **93** 140404
- [13] Yönaç M, Yu T and Eberly J H 2006 *J. Phys. B: At. Mol. Opt. Phys.* **39** S621–5
- [14] Yu T and Eberly J H 2006 *Phys. Rev. Lett.* **97** 140403
- [15] Almeida M P, de Melo F, Hor-Meyll M, Salles A, Walborn S P, Ribeiro P H S and Davidovich L 2007 *Science* **316** 579–82
- [16] Cirac J I and Zoller P 1995 *Phys. Rev. Lett.* **74** 4091–4
- [17] Monroe C, Meekhof D M, King B E, Itano W M and Wineland D J 1995 *Phys. Rev. Lett.* **75** 4714–7
- [18] Turchette Q A, Hood C J, Lange W, Mabuchi H and Kimble H J 1995 *Phys. Rev. Lett.* **75** 4710–3
- [19] Chuang I L and Yamamoto Y 1995 *Phys. Rev. A* **52** 3489–96
- [20] Knill E, Laflamme R and Milburn G J 2001 *Nature* **409** 46–52
- [21] Gilchrist A, Milburn G J, Munro W J and Nemoto K 2003 Generating optical nonlinearity using trapped atoms *Preprint* arXiv:quant-ph/0305167
- [22] Marchioli M A, Missori R J and Roversi J A 2003 *J. Phys. A: Math. Gen.* **36**, 12275–92
- [23] Marchioli M A 2006 *J. Mod. Opt.* **53** 2733–51
- [24] Azuma H 2008 *Phys. Rev. A* **77** 063820
- [25] Raizen M G, Gilligan J M, Bergquist J C, Itano W M and Wineland D J 1992 *Phys. Rev. A* **45** 6493–501
- [26] Kwiat P G, White A G, Mitchell J R, Nairz O, Weihs G, Weinfurter H and Zeilinger A 1999 *Phys. Rev. Lett.* **83** 4725–8